

Coherent Spectroscopy with Fast Frequency Swept Lasers

S. N. Andreev^a, V. N. Ochkin^a, N. V. Pestovskii^{a,b}, and S. Yu. Savinov^{a,b}

^a Lebedev Physical Institute, Russian Academy of Sciences, Moscow, 119991 Russia

^b Moscow Institute of Physics and Technology (State University), Dolgoprudny, Moscow oblast, 141700 Russia
e-mail: savinov@sci.lebedev.ru

Received January 21, 2015

Abstract—Effects caused by fast laser frequency sweeping across absorption lines are investigated. Oscillations in the time dependence of intensity of radiation generated by the medium, which are caused by beats between oscillations at variable excitation frequency and constant eigenfrequencies, are discovered. The time intervals between local maxima of the oscillations are inversely proportional to the difference between the eigenfrequency of the atomic oscillator and the instant frequency of the external radiation. The method of using fast frequency sweeping for determining indices of absorption at high optical densities ($k_0z \sim 100$) is proposed.

DOI: 10.1134/S0030400X15090027

INTRODUCTION

Effects appearing under fast frequency sweeping across an absorption line by changing applied magnetic field were first observed in the high-frequency range in studies related to NMR [1]. It was demonstrated that, upon variation of the applied magnetic field with a rate exceeding a certain threshold value, the NMR spectrum revealed oscillations that were interpreted by the authors as the result of free induction decay.

In the optical frequency range, effects appearing upon rapid passage across the absorption line were observed for the first time in [2], where optical free induction decay appearing when pulsed electric field was applied to a cell containing NH_2D gas irradiated by monochromatic radiation of a CO_2 laser was investigated. At the stage of growth and decay of the applied electric field, the pattern of decaying absorption modulated by Rabi oscillations was observed. The time constant of decay was determined by the linewidth. Using a similar technique, the effects of rapid passage across the absorption line of NH_3 caused by population inversion induced under adiabatically rapid passage through the resonance were studied in [3]. However, no oscillations were observed in this case.

In the above-mentioned works, the effects of rapid passage were realized by varying eigenfrequencies of oscillators of the medium by changing external magnetic or electric fields, while keeping the frequency of external radiation constant. The development of technology of frequency tunable lasers has created the possibility of an alternative approach. Specific features of interaction of a light field the frequency of which was

varying in the vicinity of $\lambda \approx 4.2 \mu\text{m}$ with the medium in the absence of additional fields were analyzed for the first time in [4] (see also [5]). The authors of [4] investigated the case of propagation of probe radiation exhibiting linear frequency modulation $\omega = \Omega + \mu t$, where $\Omega = \frac{\epsilon_1 - \epsilon_0}{\hbar}$ is the frequency of the studied resonance transition $|1\rangle \rightarrow |0\rangle$ and μ is the frequency sweeping rate, through an absorbing medium. In particular, it was noted that the recorded contour broadened with increasing μ , its front becoming longer, the peak of absorption was shifting, and oscillations were appearing in the tail of the contour. In so doing, in certain intervals in the area of oscillations, intensity exceeded its level in the absence of absorbing medium, i.e., intensity of the signal propagated through the medium increased. To observe these coherent phenomena, it was necessary that the characteristic time of frequency sweeping across the lines $t_{sk} = \Delta\omega/\mu$ was shorter than the characteristic coherence relaxation time in the system $\tau_F = \Delta\omega^{-1}$ (where $\Delta\omega$ is the width of the spectral line); i.e., $\mu(\Delta\omega)^{-2} = \mu\tau_F^2 > 1$. The authors developed a theoretical model of this phenomenon, which demonstrated qualitative agreement with the experiment. A detailed comparison was not conducted in [4] because, on the one hand, the frequency sweeping rates of classical injection lasers were already at the limit, and, on the other hand, the speed of recording fast signals in the IR spectral range was also limited. With the advent of fast frequency swept quantum-cascade lasers and modern means of recording spectra, many researchers returned to investigation of these effects [6–10]. In general, the results obtained

in these works were close to those described in [4], but were obtained at a higher modern level of technology, which allowed quantitative comparison of calculations with the experimental results.

When analyzing coherent phenomena, an important question is how the medium behaves under the influence of radiation. At the same time, it is not completely clear how the medium would behave under the effect of radiation with changing frequency. In the present work, we investigate specific features of coherent emission of an absorbing medium and possibilities of practical application of the technique of coherent spectroscopy for determining optical density of strongly absorbing media.

SEMICLASSICAL DESCRIPTION

Similarly to [4], we will use the semiclassical description, wherein the field of radiation is treated classically, while the medium is described as an ensemble of noninteracting two-level systems with volume density N . We assume that the beam of light is collinear and is linearly polarized. The transition moments of quantum system are assumed to be oriented in space in the direction of the polarization vector of the incident waves. The method of calculation of the electric field is similar to [4] and is based on simultaneous solution of the classical wave equation and the von Neumann equation for the two-level system. The following expression governing complex amplitude of electric field $\bar{E}(t, z)$ at the output of a cell of length z was obtained in [4]:

$$\bar{E}(t, z) = \frac{1}{2\pi} \int_{-\infty}^{\infty} d\nu \int_{-\infty}^{\infty} dt' \bar{E}(t', z=0) \times \exp\left\{i\left[\nu(t-t') - \frac{z}{c}(\nu - iA(\nu)c)\right]\right\}, \quad (1)$$

where

$$A(\nu) = \frac{2\pi k}{\hbar} |d_{10}|^2 \gamma \int_{-\infty}^{\infty} \frac{d\Delta' g(\Delta')}{\tau^{-1} - i(\Delta' - \Delta)}, \quad (2)$$

$\bar{E}(t', z=0)$ is the value of complex amplitude at the input of the cell containing the studied object, k is the absolute value of the wave vector of the probe radiation, $g(\Delta')$ is the distribution function of frequency offset (the factor that takes into account the presence of

inhomogeneous broadening $\int_{-\infty}^{\infty} g(\Delta) d\Delta = 1$), $\gamma = \gamma_0 =$

const is the population difference of combining states, and τ is the transverse relaxation time. Note that the described phenomena are not related to the dynamics of population. As a rule, the probe radiation intensity is small, and characteristic interaction time of the sys-

tem $t_{sk} = \Delta\omega/\mu$ is substantially shorter (by at least two orders of magnitude) than period $T_R = 2\pi\hbar/(E_0|d_{10}|)$ of Rabi nutations [11], where E_0 is the electric field amplitude and d_{10} is the matrix element of the dipole moment of transition $|1\rangle \rightarrow |0\rangle$.

Knowing the complex amplitude of the electric field, it is easy to calculate the radiation intensity

$$I \sim E^2 = \frac{1}{2} \bar{E}(t, z) \bar{E}^*(t, z). \quad (3)$$

We analyzed the case where the medium is subjected to the action of radiation exhibiting linear frequency modulation

$$\left. \begin{aligned} \omega &= \Omega + \mu t, & \Delta\omega - \frac{T}{2} \leq t \leq \frac{T}{2}, & T \gg \tau \\ \Delta\omega &= \mu T, & \frac{\Delta\omega}{\Omega} \ll 1 & \end{aligned} \right\}. \quad (4)$$

In the case of inhomogeneous Doppler broadening, we have

$$g(\Delta') = 2\sqrt{\frac{\ln 2}{\pi}} \frac{1}{\Delta\omega_D} \exp\left[-4 \ln 2 \left(\frac{\Delta' - \Delta}{\Delta\omega_D}\right)^2\right], \quad (5)$$

$$\Delta\omega_D = 2\tau^{-1}.$$

Optical density in the center of the line is

$$k_0 z = \frac{4\pi k |d_{10}|^2}{\hbar} \gamma z \int_{-\infty}^{\infty} \frac{\tau^{-1} g(\Delta') d\Delta'}{\tau^{-2} + \Delta'^2}. \quad (6)$$

Intensity I was calculated for time moment $t' = t - z/c$ for an absorbing cell of length z . Radiation intensity in the absence of absorption was assumed to be equal to 1.

Let us compare the results of the calculation according to the above-described approach with the experimental results obtained in [10]. The results of [10] obtained under high-speed detection of inhomogeneously broadened absorption line of NH_3 in the vicinity of $\lambda = 10 \mu\text{m}$ are illustrated in Fig. 1. The measurements were conducted under the following conditions: pressure of air- NH_3 mixture $p = 1.74$ Torr (2.32 mb), NH_3 content $c = 0.35\%$, Voigt contour of the spectral line, collisional component of broadening $\Delta\nu_L = 2.32 \times 10^{-4} \text{ cm}^{-1}$, Doppler broadening component $\Delta\nu_D = 3 \times 10^{-3} \text{ cm}^{-1}$, linewidth $\Delta\nu = 3.1 \times 10^{-3} \text{ cm}^{-1}$. The results of our calculation performed at $\mu\tau_F^2 = 2$ (dimensionless frequency sweeping rate $\mu\tau_F^2 = \tau_F/t_{sk}$) and optical density in the center of the line $k_0 z = 0.5$ are presented in the same diagram. We chose the characteristic loss of coherence time $\tau_F = \Delta\omega^{-1}$ as the unit of time. For comparison, the results of the calculation performed in [10] are also presented in Fig. 1. It can be seen that our calculation describes

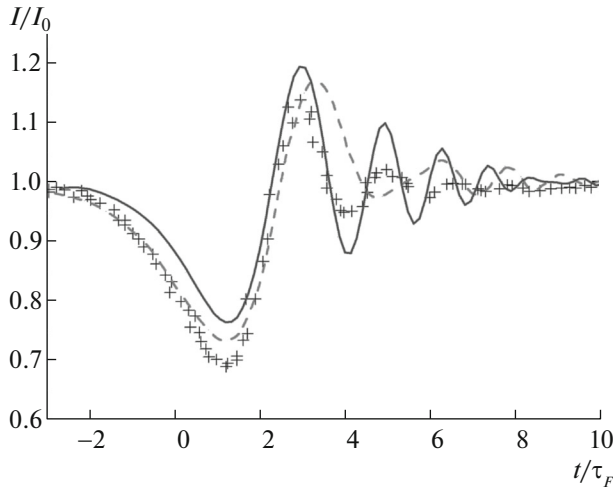


Fig. 1. Comparison of calculations and experiments conducted with high-speed acquisition for the absorption line of NH_3 in the vicinity of $\lambda = 10 \mu\text{m}$ (air- NH_3 pressure $p = 1.74$ Torr (2.32 mbar), NH_3 content $c = 0.35\%$, Voigt contour of the spectral line, collisional component of broadening $\Delta\nu_L = 2.32 \times 10^{-4} \text{ cm}^{-1}$, Doppler component of broadening $\Delta\nu_D = 3 \times 10^{-3} \text{ cm}^{-1}$, contour width $\Delta\nu = 3.1 \times 10^{-3} \text{ cm}^{-1}$ [10]): (crosses) experiment [10], (solid line) calculations made in the present work, and (dashed line) results of calculations obtained in [10].

the time evolution of the oscillations better. Apparently, this is related to the fact that the set of Bloch equations, in which taking into account the influence of inhomogeneous broadening entails enormous calculation difficulties, was used in [10]. This circumstance was noted in [12].

OSCILLATION OF COHERENT EMISSION OF AN ABSORBING MEDIUM

Field of radiation $E(t, z)$ at the output of the absorbing cell of length z can be presented as a superposition of laser field

$$E_L(t, z) = \frac{1}{2}(\bar{E}_L(t, z)e^{i(\omega t - kz)} + \text{c.c.}), \quad (7)$$

where the complex amplitude of the laser radiation is

$$\bar{E}_L(t, z) = E_0 \exp\left\{i\left(\frac{\mu t^2}{2} - \frac{\mu t z}{c} + \frac{\mu z^2}{2c^2}\right)\right\} \quad (8)$$

and field $E_{\text{med}}(t, z)$ is related to coherent emission of the medium. Then, we have

$$\bar{E}_{\text{med}}(t, z) = \bar{E}(t, z) - \bar{E}_L(t, z). \quad (9)$$

Correspondingly, the intensity of coherent emission for time moment $t' = t - z/c$ at the output of the cell of length z is

$$I_{\text{med}}(t', z) = \frac{1}{2}\{I(t', k_0 z) + 1\} - \left\{ \text{Re}[\bar{E}(t', k_0 z)] \cos\left(\frac{\mu t'^2}{2}\right) + \text{Im}[\bar{E}(t', k_0 z)] \sin\left(\frac{\mu t'^2}{2}\right) \right\}. \quad (10)$$

Here, as before, intensity in the absence of absorption was assumed to be equal to 1.

The calculated time dependences of intensity of transmitted radiation (a) and coherent emission of the medium (b) in the case of inhomogeneous broadening of spectral lines, $\sqrt{\ln 2} \frac{\Delta\omega_{\text{hom}}}{\Delta\omega_D} = 0.1$, $\Delta\omega_{\text{hom}} = 2\tau^{-1}$ are presented in Figs. 2 and 3. Figure 2 corresponds to dimensionless frequency sweeping rate $\mu\tau_F^2 = 3.21$, while Fig. 3 corresponds to $\mu\tau_F^2 = 6.42$. The value of optical density at the center of the line is $k_0 z = 0.5$. The obtained time dependence of intensity of the transmitted radiation (Figs. 2a and 3a) corresponds to the expected one. The maximum of absorption is shifted, and oscillations of intensity are observed in the tail of the contour. In some zones in the region of oscillations, intensity exceeds its value in the absence of the absorbing medium, i.e., the signal intensity increases. The behavior of intensity of coherent emission of the medium (Figs. 2b and 3b) appearing as a result of action of external radiation of variable frequency is of interest. Characteristic oscillations are also observed in the pulse tail. We believe that, physically, the onset of oscillations is explained as follows. When absorption is weak, the sample can be considered as a set of phased radiation dipoles (superradiant state of the system [13]). They emit coherent radiation that propagates within a solid angle determined by the original laser radiation. Oscillations of each oscillator in the case under consideration represent a superposition of eigenoscillations at frequency Ω and driven oscillations at frequency ω of the external action. The frequency of the external action is variable, and the phase difference of free and driven oscillations is determined

by quantity $\frac{\mu t^2}{2}$. Correspondingly, one can expect that distance $(t_2 - t_1)$ between secondary maxima in the time dependence of intensity of coherent emission of the medium must be determined from the condition

$$\frac{\mu(t_2^2 - t_1^2)}{2} = 2\pi, \text{ i.e.,}$$

$$\mu = \frac{4\pi}{(t_2 - t_1)(t_2 + t_1)}, \quad (11)$$

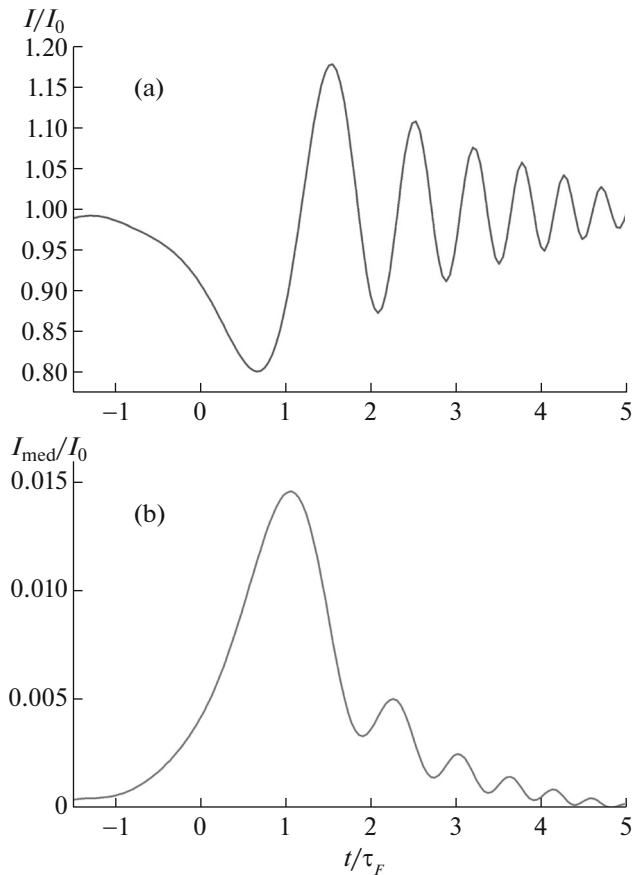


Fig. 2. Calculated time dependences of transmitted radiation (a) and coherent emission of the medium (b). $\mu\tau_F^2 = 3.21$, $k_0z = 0.5$.

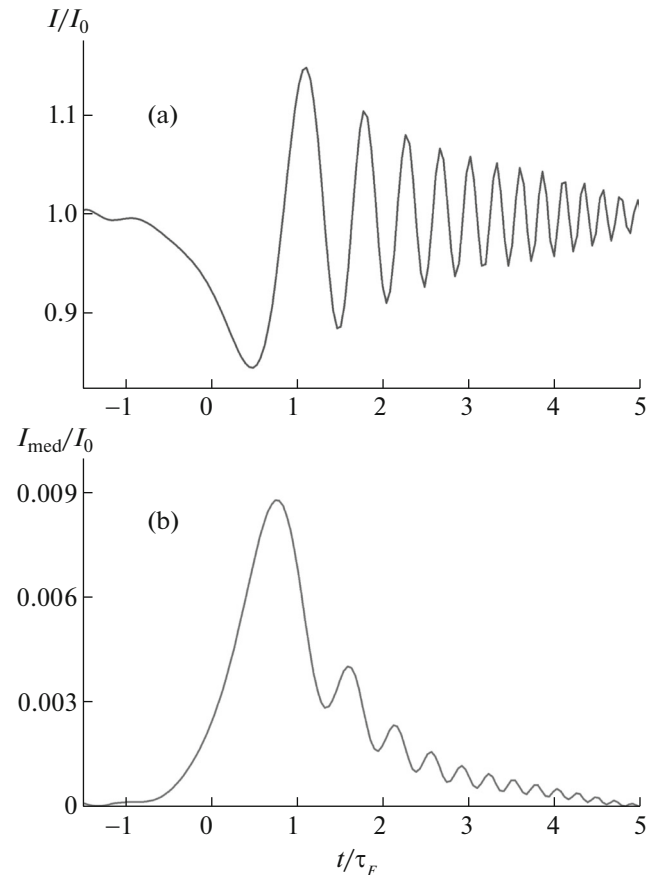


Fig. 3. Calculated time dependences of transmitted radiation (a) and coherent emission of the medium (b). $\mu\tau_F^2 = 6.42$, $k_0z = 0.5$.

which agrees well with the presented calculations. For instance, for the case presented in Fig. 2, the dimensionless frequency sweeping rate determined from (10) is $\mu\tau_F^2 = 3.11$, $t_2 = 3.03$, and $t_1 = 2.27$ (exact value is $\mu\tau_F^2 = 3.21$); for the case presented in Fig. 3, $\mu\tau_F^2 = 6.38$, $t_2 = 2.13$, and $t_1 = 1.65$ (exact value is $\mu\tau_F^2 = 6.42$). Correspondingly, the time intervals between the local maxima are inversely proportional to the difference between the eigenfrequency of the atomic oscillator and the instant frequency of the external radiation $(t_2 - t_1) \sim [\omega(t) - \Omega]^{-1} = (\mu t)^{-1}$.

In the case of strong absorption, the observed pattern is more complicated. The calculated dependences of intensity of transmitted radiation (a) and coherent emission of the medium (b) for the case of line center absorption $k_0z = 10$ are presented in Fig. 4 (dimensionless frequency sweeping rate $\mu\tau_F^2 = 3.21$) and Fig. 5 (dimensionless frequency sweeping rate $\mu\tau_F^2 = 6.42$). It can be seen that radiation is passing through the medium, despite high value of the optical

density. Comparison with Figs. 2 and 3 shows that intensities of transmitted radiation and coherent emission of the medium considerably increase with increasing index of absorption. This result is related to increased number of particles participating in energy exchange with the radiation field, which leads to increased contribution of the coherent emission of the medium. Coherent emission of the medium appears in the form of a pulse train. Such complex behavior is caused by the fact that coherent emission of individual regions of the medium is formed as a result of action of not only external probe radiation but also coherent emission of other regions of the medium corresponding to smaller values of z [14].

FINDING OPTICAL DENSITY AT HIGH VALUES OF THE INDEX OF ABSORPTION

Comparison of results presented in Figs. 4 and 5 shows that variation of k_0z causes very large changes in the time dependences of radiation intensities. This circumstance can be used for finding k_0z [15]. In partic-

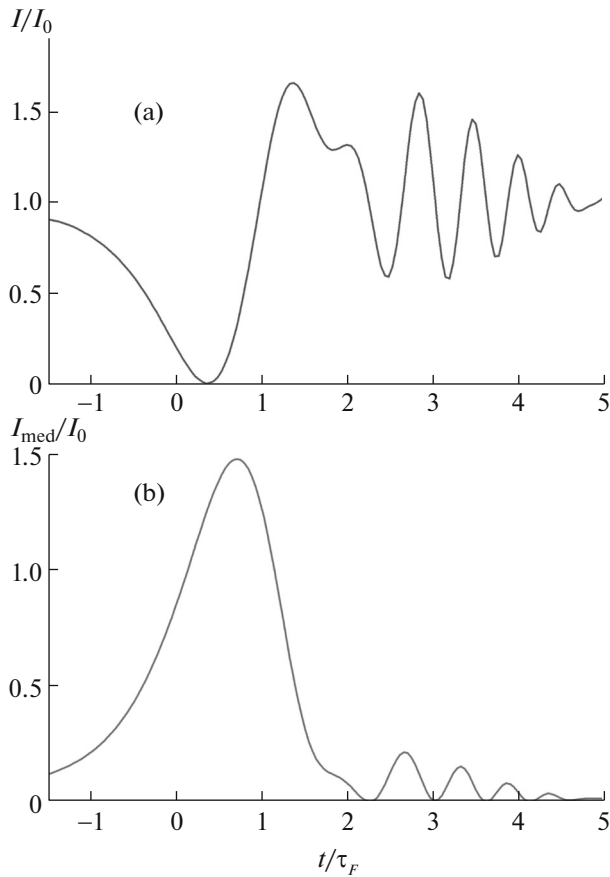


Fig. 4. Calculated time dependences of transmitted radiation (a) and coherent emission of the medium (b). $\mu\tau_F^2 = 3.21$, $k_0z = 10$.

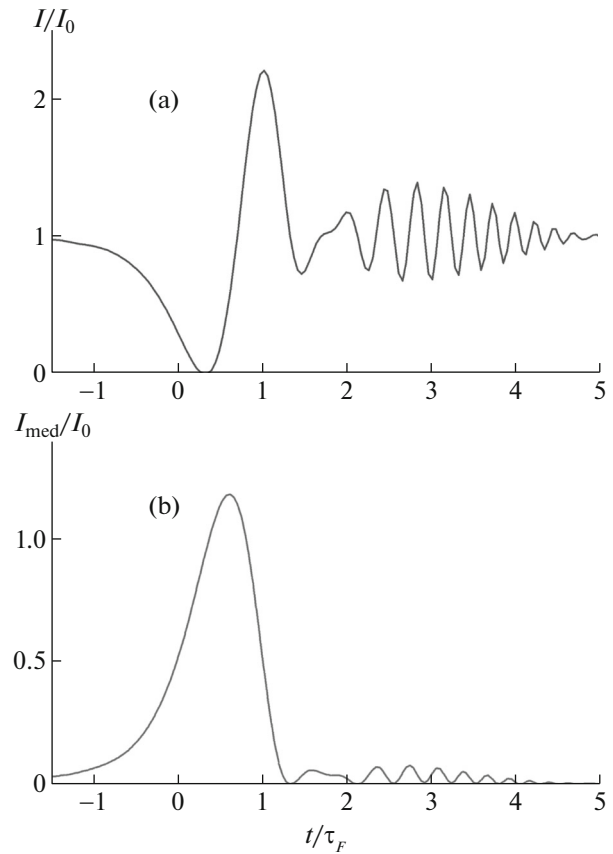


Fig. 5. Calculated time dependences of transmitted radiation (a) and coherent emission of the medium (b). $\mu\tau_F^2 = 6.42$, $k_0z = 10$.

ular, this seems to be of interest for determining k_0z in weakly transmitting media, when measurements of absorption require measuring intensities with high accuracy [16]. Figure 6 illustrates spectral transmission for a Doppler contour corresponding to $k_0z = 0.5, 2, 5, 40,$ and $95-105$ (the Bouguer–Lambert–Beer law):

$$I(x)/I_0 = \exp\{-k_0zF_D(x)\}, \quad (12)$$

where $F_D(x) = \exp\{-4\ln 2x^2\}$, $x = \Delta\omega/\Delta\omega_D$, $\Delta\omega_D$ is the Doppler width of the spectral line, and I_0 is the laser source intensity (the latter is assumed to be constant in the vicinity of the absorption line). The dependences of this kind are traditionally used in classical spectroscopy, where frequency of the external source is varied slowly.

It can be seen from Fig. 6 that, for indices of absorption $k_0z \geq 5$, dependence (12) saturates in the vicinity of the absorption line, while, at $k_0z \geq 50$, the difference between the curves is small even in the wings of the absorption curves. For quantitative esti-

mate of the difference between the transmission curves, let us introduce quantity R defined as

$$R(k_0z, (k_0z)^*) = \frac{1}{\sqrt{n}} \sqrt{\sum_n \left[\frac{I_i(k_0z)}{I_0} - \frac{I_i((k_0z)^*)}{I_0} \right]^2}. \quad (13)$$

When calculating this quantity, all dependences were divided into n intervals and the value of R was found as the average mean-squared deviation of the transmission curve corresponding to index k_0z from the transmission curve corresponding to index of absorption $(k_0z)^*$. The calculated dependences $R((k_0z), (k_0z)^*)$ are presented in Fig. 7. Curve 1 corresponds to $(k_0z)^* = 100$ and $n = 281$. It can be seen that R exceeds 0.1 (10%) when k_0z varies between 10 and 40. However, in the vicinity of $k_0z \sim 100$, this quantity is small, e.g., for $(k_0z) = 95$ or $(k_0z) = 105$, we have $R = 6.7 \times 10^{-3}$ or $R = 6.4 \times 10^{-3}$. In practice, k_0z can be found by comparing the experimental curve with those calculated from (12) and minimizing the value of $R((k_0z)^{\text{exp}}, (k_0z)^{\text{calc}})$ (13). Consequently, to ensure 5% uncertainty of determining k_0z in the region of high

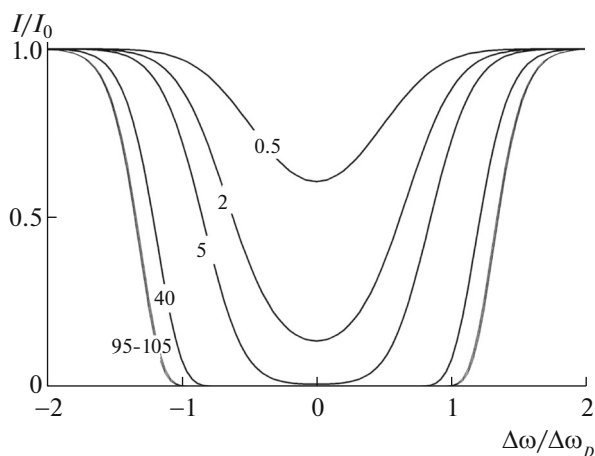


Fig. 6. Spectral transmission for a Doppler contour for $k_0z = 0.5, 2, 5, 40,$ and $95-105$ (Bouguer–Lambert–Beer law).

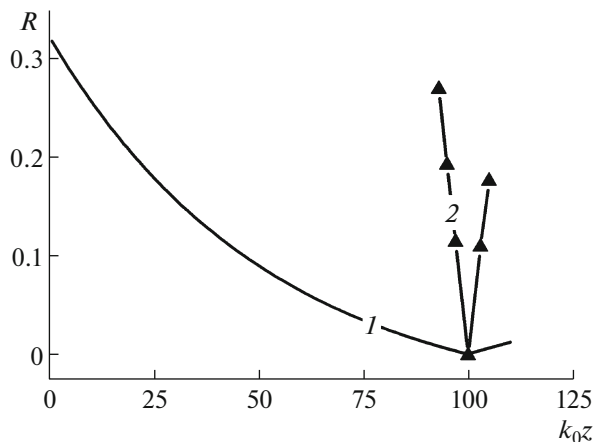


Fig. 7. Calculated dependence $R(k_0z, (k_0z)^*)$ at $(k_0z)^* = 100$ and $n = 281$: (1) using the Bouguer–Lambert–Beer law, (2) fast frequency sweeping across the absorption line ($\mu\tau_F^2 = 3.21$).

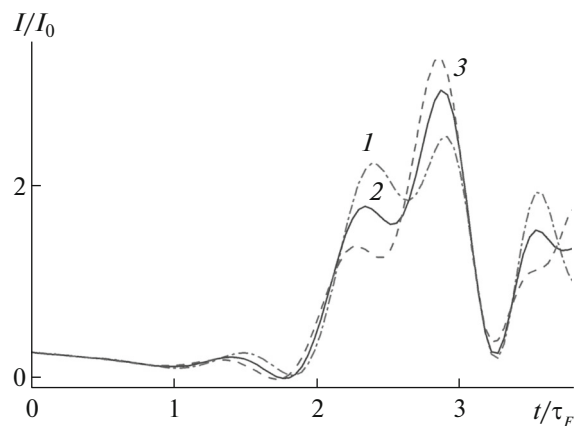


Fig. 8. Calculated time dependences of transmitted radiation for $\mu\tau_F^2 = 3.21$; $k_0z = (1) 95, (2) 100,$ and $(3) 105$.

absorption ($k_0z \sim 100$), the uncertainty of measuring intensity must be $\frac{\Delta I}{I_0} \approx 0.2\%$ (this corresponds to the level of $1/3R$), which is not always easy to do.

We compared the time dependences of intensity of transmitted radiation (3) for $k_0z = 95, 100,$ and 105 for the case of inhomogeneously broadened spectral lines:

$$\sqrt{\ln 2} \frac{\Delta\omega_{\text{hom}}}{\Delta\omega_D} = 0.1, \Delta\omega_{\text{hom}} = 2\tau^{-1},$$

obtained under fast frequency sweeping across the absorption line (the dimensionless frequency sweeping rate $\mu\tau_F^2 = 3.21$) (Fig. 8). This corresponds to the spectral lines of the fundamental absorption band of CO_2 molecules in the vicinity of $4.3 \mu\text{m}$ at pressure $p \sim 1$ Torr and temperature $T = 300$ K. Calculated values of $R((k_0z), (k_0z)^*)$ for $(k_0z)^* = 100$ and $n = 281$ are presented by curve 2 in Fig. 7. For $k_0z = 93, 95, 97, 103,$ and 105 , the corresponding values of the averaged normalized mean squared deviations are $R = 0.270, 0.193, 0.15, 0.11,$ and 0.177 , respectively. When using this method for finding the indices of absorption in practice, it is necessary to compare the experimental time dependence of intensity of transmitted radiation with calculated dependences (3), minimizing the value of R by varying only parameter k_0z , similar to the technique based on using the Bouguer–Lambert–Beer law. However, in the latter case, to achieve 5% uncertainty of determining k_0z in the region of strong absorption ($k_0z \sim 100$), it is sufficient to measure intensity with uncertainty $\frac{\Delta I}{I_0} \approx 6\%(1/3R)$.

CONCLUSIONS

We analyzed the process of interaction of the light field of variable frequency with an absorbing medium in the case of fast frequency sweeping across the absorption line. The role of coherent emission of the medium, which has an oscillating character, is revealed.

In the case of small values of optical density, oscillations are caused by the superposition of eigenoscillations of an atomic oscillator and driven oscillations of the latter under the influence of the field of varying frequency. The time intervals between the local maxima of oscillations are inversely proportional to the difference between eigenfrequency of the atomic oscillator and instant frequency of the external radiation.

With increasing index of absorption, the intensities of transmitted radiation and coherent emission of the medium considerably increase.

In the case of high optical density, oscillations are caused by the fact that coherent emission of specific regions of the medium is formed not only under the influence of the external probe radiation but also under the influence of coherent emission of other

regions of the medium corresponding to smaller values of z .

The method of using fast frequency sweeping for determining indices of absorption at high optical densities ($k_0 z \sim 100$) is proposed.

ACKNOWLEDGMENTS

This work was supported by the Russian Foundation for Basic Research, project no. 14-02-00784.

REFERENCES

1. N. Bloembergen, E. M. Purcell, and R. V. Pound, *Phys. Rev.* **73** (7), 679 (1948).
2. R. G. Brewer and R. L. Shoemaker, *Phys. Rev. A* **6** (6), 2001 (1972).
3. M. M. T. Loy, *Phys. Rev. Lett.* **32** (15), 814 (1974).
4. I. I. Zasavitskii, M. A. Kerimkulov, A. I. Nadzhedinskii, V. N. Ochkin, S. Yu. Savinov, M. V. Spiridonov, and A. P. Shotov, *Opt. Spektrosk.* **65**, 1198 (1988).
5. V. N. Ochkin, *Spectroscopy of Low Temperature Plasma* (Wiley-VCH, New York, 2009).
6. E. Normand, M. McCulloch, G. Duxbury, and N. Langford, *Opt. Lett.* **28** (1), 16 (2003).
7. M. T. McCulloch, E. L. Normand, N. Landford, and G. Duxbury, *J. Opt. Soc. Am.* **20** (8), 1761 (2003).
8. G. Duxbury, J. F. Kelly, T. A. Blake, and N. Landford, *J. Chem. Phys.* **136**, 174319 (2012).
9. S. Zamith, J. Degert, S. Stock, and B. Beauvior, *Phys. Rev. Lett.* **87** (3), 033001 (2001).
10. B. Grouiez, V. Zeninari, L. Joly, and B. Parvitte, *Appl. Phys.* **100**, 265 (2010).
11. L. D. Landau, and E. M. Lifshits, *Quantum Mechanics* (Nauka, Moscow, 1974) [in Russian].
12. M. T. McCulloch, G. Duxbury, and N. Landford, *Mol. Phys.* **104** (16–17), 2767 (2006).
13. R. H. Dicke, *Phys. Rev.* **93**, 99 (1954).
14. S. N. Andreev, A. V. Mikhailov, V. N. Ochkin, N. V. Pestovskiy, and S. Yu. Savinov, *Las. Phys.* **25**, 1 (2015).
15. S. N. Andreev, A. V. Mikhailov, V. N. Ochkin, N. V. Pestovskiy, and S. Yu. Savinov, *J. Russ. Las. Res.* **36** (2), 119 (2015).
16. V. N. Ochkin, *Problems of Optical Technique for Diagnostics of Objects by Relative Content of Stable Isotopes* (FIAN, Moscow, 2012).